

## Extensive and Subextensive Chaos in Globally Coupled Dynamical Systems

Kazumasa A. Takeuchi,<sup>1,2</sup> Hugues Chaté,<sup>1</sup> Francesco Ginelli,<sup>3,4,5,1</sup> Antonio Politi,<sup>6,5</sup> and Alessandro Torcini<sup>6,4</sup>

<sup>1</sup>*Service de Physique de l'État Condensé, CEA-Saclay, F-91191 Gif-sur-Yvette, France*

<sup>2</sup>*Department of Physics, The University of Tokyo, 7-3-1 Hongo, Bunkyo-ku, Tokyo 113-0033, Japan*

<sup>3</sup>*CNR, Istituto dei Sistemi Complessi (ISC), Via dei Taurini 19, I-00185 Roma, Italy*

<sup>4</sup>*Dipartimento di Fisica and INFN, Università di Firenze, Via Sansone 1, I-50019 Sesto Fiorentino, Italy*

<sup>5</sup>*Department of Physics and SUPA, University of Aberdeen, Aberdeen AB24 3UE, United Kingdom*

<sup>6</sup>*CNR, Istituto dei Sistemi Complessi, via Madonna del Piano 10, I-50019 Sesto Fiorentino, Italy*

(Received 23 March 2011; published 13 September 2011)

Using a combination of analytical and numerical techniques, we show that chaos in globally coupled identical dynamical systems, whether dissipative or Hamiltonian, is both extensive and subextensive: their spectrum of Lyapunov exponents is asymptotically flat (thus extensive) at the value  $\lambda_0$  given by a single unit forced by the mean field, but sandwiched between subextensive bands containing typically  $\mathcal{O}(\log N)$  exponents whose values vary as  $\lambda \simeq \lambda_\infty + c/\log N$  with  $\lambda_\infty \neq \lambda_0$ .

DOI: 10.1103/PhysRevLett.107.124101

PACS numbers: 05.45.-a, 05.45.Xt, 05.70.Ln, 05.90.+m

Dynamical systems made of many coupled units with long-range or global coupling are models of numerous important situations in physics and beyond, ranging from the synchronization of oscillators and neural networks to gravitational systems, plasma, and hydrodynamics [1,2]. Their properties can be quite remarkable: for instance, globally coupled dissipative systems can give rise to collective chaos, where macroscopic variables show incessant irregular behavior due to nontrivial correlations between local units [3]. Their Hamiltonian counterparts, in the microcanonical ensemble, are now well known to show negative specific heat, long-lived quasistationary states, all features ultimately related to their nonadditivity [1]. Their unusual properties make these systems deceptively close to simple mean-field approximations and less well understood than systems with short-range interactions.

Particularly unclear is the status of the chaos. For systems with short-range interactions, Ruelle [4] conjectured extensivity of chaos, arguing that a sufficiently large spatial domain can be divided into small, practically independent subsystems with similar dynamic properties. Extensivity is customarily probed by studying the finite-size scaling properties of Lyapunov exponents (LEs). When LEs  $\lambda^{(i)}$ , arranged in descending order and plotted as functions of  $(i - \frac{1}{2})/N$ , collapse onto a single asymptotic spectrum for large-enough system sizes  $N$ , chaos is deemed extensive. This has been observed repeatedly in locally coupled systems [5] (at least in the absence of collective modes, which are nonextensive [6]), but there is, in our view, no solid evidence or argument for or against the extensivity of chaos in long-range or globally coupled systems, even with the system sizes reachable numerically today (see, e.g., Fig. 2(a) below).

Yet, a naive argument suggests extensivity in this latter case: for identical units submitted to the same

self-consistent forcing, the influence of a given unit on the mean field vanishes in the thermodynamic limit and hence the LEs should all take the same value (hereafter  $\lambda_0$ ), a trivial realization of extensivity. But this is strictly true only if the  $N \rightarrow \infty$  limit is taken first, which may be misleading when dealing with LEs, as they are essentially infinite-time averages. In fact, the Lyapunov spectra of finite-size globally coupled systems always remain far from being flat [see again Fig. 2(a)].

For the paradigmatic and much-studied Hamiltonian mean-field (HMF) model [7,8], the situation is similarly confusing: the naive argument above gives all LEs at zero, whereas a calculation by Firpo yielded a positive largest exponent at any finite  $N$ , with a well-defined  $N \rightarrow \infty$  limit [9]. A theoretical formulation as a quantum many-body problem mentioned the possibility of a vanishing fraction of nonzero exponents [10], but numerical results have produced contradictory results [8,11].

In this Letter, we show that chaos is not fully extensive in systems of globally coupled identical units. Rather, their Lyapunov spectra, in the large-size limit, converge to flat extensive regions where the LEs do take the value  $\lambda_0$  given by the single unit forced by the mean field, but these regions are bordered by subextensive layers containing exponents taking different values. In particular, we provide a theoretical analysis and numerical evidence showing that the largest LE  $\lambda^{(1)}$  converges as  $\lambda^{(1)} \simeq \lambda_\infty + c/\log N$  to an asymptotic value  $\lambda_\infty > \lambda_0$ . Our numerical analysis reveals that the subextensive boundary layers contain  $\mathcal{O}(\log N)$  Lyapunov modes and that their LEs take the same asymptotic value  $\lambda_\infty$ .

We first study  $N$  globally coupled dissipative maps

$$x_j^{t+1} = f(y_j^t), \quad y_j^t = (1 - \varepsilon)x_j^t + \frac{\varepsilon}{N} \sum_{j'=1}^N x_{j'}^t, \quad (1)$$

with  $j = 1, \dots, N$ , time  $t$ , coupling constant  $\varepsilon$ , and a chaotic local map  $f(x)$ , which is chosen here to be one-dimensional for the sake of simplicity. If  $f(x)$  shows sufficiently strong mixing, its Jacobian may be approximated by a random multiplier. The tangent-space dynamics of Eq. (1) is then simplified as

$$v_j^{t+1} = \mu_j^t \left[ (1 - \varepsilon)v_j^t + \frac{\varepsilon}{N} \sum_{j'=1}^N v_{j'}^t \right], \quad (2)$$

with independent identically distributed random numbers  $\mu_j^t$ , unless the coupling  $\varepsilon$  is too strong to regard  $f'(y_j^t)$  as independent. The mean-field forcing argument amounts to ignoring the global-coupling term in Eq. (2), which is then reduced to the biased Brownian motion of a particle of coordinate  $\log|v_j^t|$  with average velocity  $\lambda_0 \equiv \langle \log|(1 - \varepsilon)\mu_j^t| \rangle$  and diffusion coefficient  $D \equiv \langle (\log|(1 - \varepsilon)\mu_j^t| - \lambda_0)^2 \rangle$ , where  $\lambda_0$  is the mean-field LE. From this viewpoint, the full system (2) can be seen as  $N$  interacting Brownian particles. Assume now that the Lyapunov vector  $[v_1^t, \dots, v_N^t]$  is sufficiently localized, which is indeed the case except when it is associated with collective behavior [6]. In this case, its largest component  $v_M^t$  dominates the coupling term in Eq. (2). Thus, the Brownian particles  $\log|v_j^t|$  diffuse freely as long as  $|(1 - \varepsilon)v_j^t| \gg |(\varepsilon/N)v_M^t|$ , otherwise the coupling term takes effect, keeping any  $|(1 - \varepsilon)v_j^t|$  larger than  $|(\varepsilon/N)v_M^t|$ . In other words, the  $N$  Brownian particles  $\log|v_j^t|$  diffuse within a box of size  $\log[N(1 - \varepsilon)/\varepsilon]$ , whose right end corresponds to the rightmost particle, while the other end pulls all the particles left behind. The first LE  $\lambda^{(1)}$  is then simply given as the average velocity of this box. This process is described by the following Fokker-Planck equation in a frame moving at velocity  $\lambda^{(1)}$ :

$$\frac{\partial}{\partial t} P(u, t) = -\frac{\partial}{\partial u} [(\lambda_0 - \lambda^{(1)})P] + \frac{D}{2} \frac{\partial^2 P}{\partial u^2}, \quad (3)$$

where  $u$  is the coordinate in this frame and the particle distribution function  $P(u, t)$  is confined, roughly, in  $0 \leq u \leq u_{\max} \equiv \log[N(1 - \varepsilon)/\varepsilon]$ . For large  $N$ , its stationary solution can be approximated by the one in the limit  $u_{\max} \rightarrow \infty$ ,  $P_s(u) = (2\Delta\lambda^{(1)}/D) \exp(-2\Delta\lambda^{(1)}u/D)$  with  $\Delta\lambda^{(1)} \equiv \lambda^{(1)} - \lambda_0$ . Further, by the definition of the box, there should be  $\mathcal{O}(1)$  particles near its right end  $u_{\max}$ , which implies  $\int_{u_{\max}}^{\infty} P_s(u) du = c_1/N$  with a constant  $c_1 \sim \mathcal{O}(1)$ . This yields our central result for the first LE:

$$\Delta\lambda^{(1)} = \lambda^{(1)} - \lambda_0 = \frac{D}{2} \left( 1 + \frac{c_2}{\log N} \right) + \mathcal{O}\left(\frac{1}{\log^2 N}\right), \quad (4)$$

with  $c_2 \equiv \log[\varepsilon/(1 - \varepsilon)c_1]$ . The probability distribution  $\mathcal{P}(v)$  for the vector components  $v_j$  is  $\mathcal{P}(v) = P_s(\log v) \times (du/dv) \sim v^{-2-c_2/\log N}$ , whose exponent is smaller than  $-1$  and thus consistent with our assumption of localization

of the Lyapunov vector. A similar result holds for the last LE:  $\Delta\lambda^{(N)} \equiv \lambda^{(N)} - \lambda_0 \simeq -(D/2)(1 + c_2'/\log N)$  with another coefficient  $c_2'$ .

These results are confirmed in Fig. 1 by direct simulations of the random multiplier (RM) model (2) and of globally coupled maps (GCM) (1) [12].

For the RM model, we used  $\varepsilon = 0.1$  and  $\mu_j^t = \pm \exp[\xi_j^t/(1 - \varepsilon)]$  with random signs (here “+” with probability 0.6) and  $\xi_j^t$  drawn from the centered Gaussian with variance  $a^2$ , which gives  $\lambda_0 = 0$  and  $D = a^2$ . Quantitative agreement is found with Eq. (4) for the first LE and its counterpart for the last LE [Figs. 1(a) and 1(c)].

For our GCM system, we chose skewed-tent maps  $f(x) = bx$  [ $b(x - 1)/(1 - b)$ ] if  $0 \leq x \leq 1/b$  [ $1/b < x \leq 1$ ] coupled with strength  $\varepsilon = 0.02$ . The results in Fig. 1(b) demonstrate again the logarithmic size dependence of  $\Delta\lambda^{(1)}$  and  $\Delta\lambda^{(N)}$ . Their asymptotic values are not symmetric anymore [Fig. 1(b)], but the deviation from  $D/2$  remains small [Fig. 1(c)]. In addition, we note that here  $\lambda_0$  depends residually on  $N$  through changes in the invariant measure. This effect is, however, so weak that in practice we observe the same logarithmic law for the first and last LEs,  $\lambda^{(1)}$  and  $\lambda^{(N)}$ .

Let us summarize our results so far: The first and last LEs remain distinct from the mean-field forcing LE  $\lambda_0$  in the  $N \rightarrow \infty$  limit. They are shifted by an amount  $\Delta\lambda$  controlled by  $D$ , or the amplitude of the fluctuations in the Jacobian, and the coupling strength  $\varepsilon$  is only involved in the logarithmic finite-size corrections [13].

We now investigate the full Lyapunov spectrum of our systems. As seen above, it cannot be entirely flat at  $\lambda_0$  asymptotically. However, for finite-size systems, Lyapunov spectra become flatter for larger sizes under the conventional rescaling  $\lambda^{(i)}$  vs  $h \equiv (i - \frac{1}{2})/N$  [Fig. 2(a)]. In

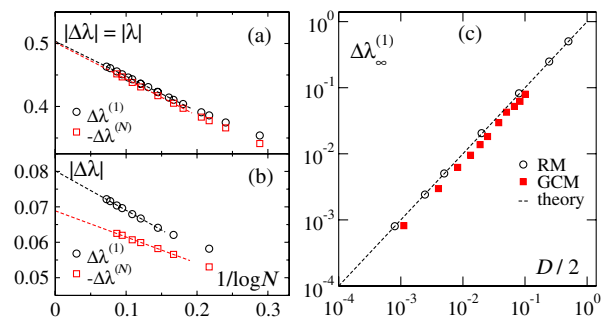


FIG. 1 (color online). Size dependence of the first and last LEs [12]. (a), (b)  $\Delta\lambda^{(1)}$  and  $|\Delta\lambda^{(N)}|$  against  $1/\log N$  for the RM model with  $a = 1$  (a) and for the skewed-tent GCM with  $b = 4$  (b). Dashed lines indicate linear fits to the data. (c) Estimated value of  $\Delta\lambda_{\infty}^{(1)} = \lim_{N \rightarrow \infty} \Delta\lambda^{(1)}$  for the RM model and our GCM with varying  $a$  and  $b$ , respectively, plotted against  $D/2$ . The diffusion constant  $D$  is obtained by  $D = a^2$  for the RM model and numerically measured for the GCM. Dashed line:  $\Delta\lambda_{\infty}^{(1)} = D/2$  as predicted in Eq. (4).

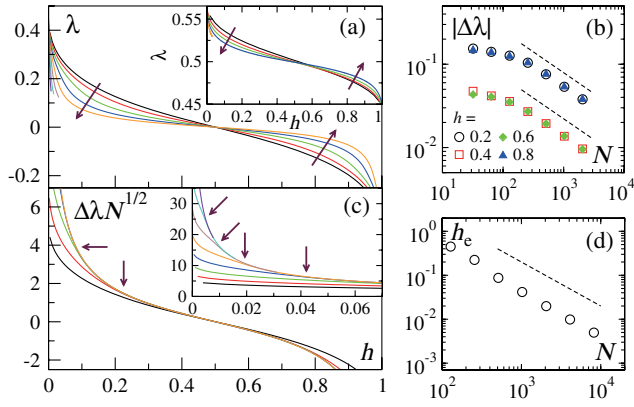


FIG. 2 (color online). Full Lyapunov spectrum for the RM model with  $a = 1$  [12]. (a) Spectra for different sizes (arrows: increasing  $N$ ) for the RM model (main panel,  $N = 128, 256, 512, \dots$ ) and for the skewed-tent GCM with  $b = 4$  (inset,  $N = 32, 128, 512, \dots$ ). (b)  $|\Delta\lambda|$  vs  $N$  at fixed values of  $h$ . Dashed lines:  $|\Delta\lambda| \sim 1/\sqrt{N}$ . (c) Same data as in main panel of (a) in rescaled coordinate from  $N = 128$  (main panel, innermost curve) to  $N = 16384$  (inset, outermost curve). Arrows indicate the positions  $h_e(N)$  at which spectra of size  $N$  and  $2N$  start to collapse. (d)  $h_e(N)$  vs  $N$ . Dashed line:  $h_e(N) \sim 1/N$ .

the RM model, a closer look at the “bulk” LEs with fixed  $h$  reveals an asymptotic power-law decay  $\Delta\lambda(h) \equiv \lambda^{(i)} - \lambda_0 \sim 1/\sqrt{N}$  toward the mean-field forcing value  $\lambda_0 = 0$  [Fig. 2(b)]. This scaling is only reached for large-enough sizes and sooner near the middle of the spectrum, as shown clearly by rescaled spectra  $\Delta\lambda\sqrt{N}$  [Fig. 2(c)]: they collapse very well within a central region  $[h_e(N), 1 - h_e(N)]$ , with  $h_e(N)$  decreasing toward zero as  $1/N$  [Fig. 2(c) arrows and Fig. 2(d)]. Thus, in the infinite-size limit, the Lyapunov spectrum of the RM model is indeed flat at  $\lambda_0$ , but sandwiched between two subextensive bands of LE taking different values [14].

That  $h_e \sim 1/N$  [Fig. 2(d)] implies that the number of nonextensive LEs increases slower than any power of  $N$ . We now show that it actually grows logarithmically with  $N$ . With fixed indices  $i$ , these LEs at size  $N$  seem to obey Eq. (4),  $\lambda_N^{(i)} \simeq \lambda_\infty^{(i)} + c^{(i)}/\log N$  [Fig. 3(a)], but the estimated  $\lambda_\infty^{(i)}$  increase with  $i$  (dashed lines), at odds with the monotonicity of the Lyapunov spectrum. This is better seen when plotting  $(\lambda_{2N}^{(i)} \log 2 - \lambda_N^{(i)} \log N)/\log 2$  as estimates for  $\lambda_\infty^{(i)}$  [inset of Fig. 3(a)], where  $\lambda_\infty^{(i)}$  is found to be larger than  $\lambda_\infty^{(1)}$  within the nonextensive region  $1 \leq i \leq i_e \equiv h_e N$ . Instead, if we rescale the index logarithmically as  $h' \equiv (i - 1)/(i_0 + \log N)$ , with  $i_0$  adjusted here for the LEs to show the  $1/\log N$  law, the asymptotic LEs  $\lambda_\infty(h')$  do not increase with  $h'$  anymore, but stay constant in the nonextensive region except near the threshold [Fig. 3(b), left of the dashed line]. This indicates that all the nonextensive LEs converge to the same value as the first LE and that their number increases logarithmically with  $N$ . The same conclusion is reached for our GCM system [Figs. 3(c)

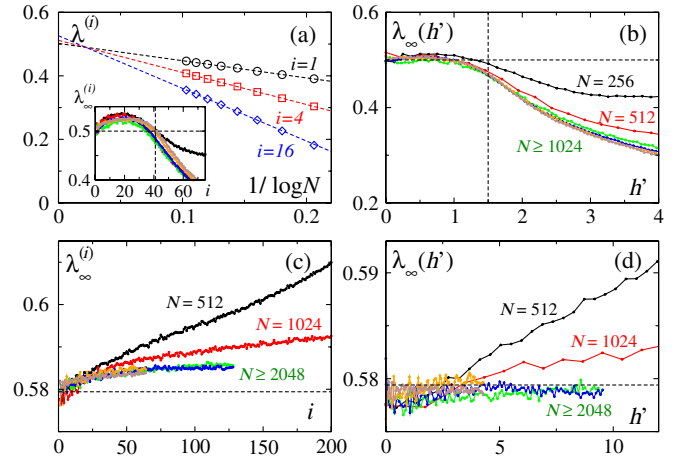


FIG. 3 (color online). Left subextensive band of the Lyapunov spectrum for the RM model with  $a = 1$  (a),(b) and for the skewed-tent GCM with  $b = 4$  (c),(d) [12]. (a)  $\lambda^{(i)}$  vs  $1/\log N$  for  $i = 1, 4, 16$ . Dashed lines indicate linear fits to the data. Inset:  $\lambda_\infty^{(i)} \equiv (\lambda_{2N}^{(i)} \log 2 - \lambda_N^{(i)} \log N)/\log 2$  vs  $i$  for  $N = 256, 512, \dots, 8192$  (see text). The horizontal and vertical dashed lines indicate  $\lambda_\infty^{(1)}$  and a threshold index value estimated from  $h_e$ , respectively. (b) Same plot as the inset of (a) but with rescaled indices  $h' \equiv (i - 1)/(i_0 + \log N)$  with  $i_0 = 15$ . (c),(d) Same plots as the inset of (a) and (b) for the GCM with  $N = 512, 1024, \dots, 16384$ , and  $i_0 = 5$ .

and 3(d)], though we could not compute all the nonextensive LEs within a reasonable time [12]. In short, we find that  $\mathcal{O}(N)$  extensive LEs are sandwiched by two subextensive bands at both ends of the spectrum, each of which consists of  $\mathcal{O}(\log N)$  LEs with asymptotic values shifted approximately by  $D/2$  from  $\lambda_0$ .

We now show that our results also extend to the HMF model, and thus probably also to other globally coupled Hamiltonian models. Defined by the Hamiltonian  $H = \frac{1}{2} \sum_j p_j^2 + \frac{1}{2N} \sum_{j,j'} [1 - \cos(\theta_j - \theta_{j'})]$ , the HMF model is intensely studied mostly because its infinite-size limit displays an abundance of nontrivial solutions which appear as so-called quasistationary states at finite  $N$  [7,8]. Contradictory results exist about the nature of chaos in this model [8,11], even in its reference “equilibrium” state. The motion of a single particle is given by  $\ddot{\theta}_j = -M \sin(\theta_j - \Theta)$ , where  $M e^{i\Theta} \equiv \frac{1}{N} \sum_j e^{i\theta_j}$  is the mean field which is nonzero in the (equilibrium) ferromagnetic phase present for energy density  $U < \frac{3}{4}$ . Here the naive argument yields  $\lambda_0 = 0$  because a single particle forced by a constant mean field cannot be chaotic.

We were able to extend the argument leading to Eq. (4) to the HMF model (details will appear elsewhere [15]): At finite  $N$ , the mean field fluctuates and the energy of a particle diffuses, so that it eventually visits the surroundings of  $U_M = 1 + M$ , the unstable maximum of the mean-field potential. There, it experiences a chaotic kick, and this produces a finite diffusion coefficient  $D$  for the logarithm of the tangent-space amplitudes. Taking these effects into

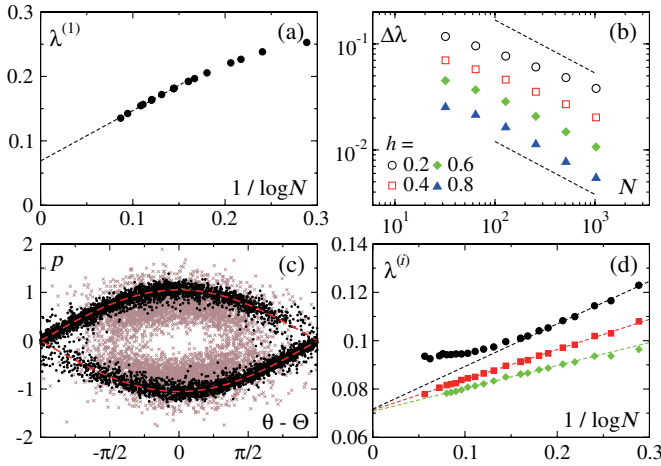


FIG. 4 (color online). (a)–(c) HMF model with energy density  $U = 0.7$  [12]. (a) First LE, maximum size  $N = 10^5$ . Dashed line: linear fit in the  $1/\log N$  regime. (b)  $\Delta\lambda$  ( $= \lambda$ ) vs  $N$  at fixed rescaled indices  $h$ . Dashed lines:  $\Delta\lambda \sim 1/\sqrt{N}$ . (c) Positions of the oscillator most contributing to the 1st and 256th Lyapunov vector (black dots and brown crosses, respectively) at  $N = 512$ . Red dashed line indicates the separatrix. (d) First 3 LEs for globally coupled Hopf oscillators (see text). Dashed lines: linear fits in the  $1/\log N$  regime.

account, we obtain a strictly positive asymptotic first LE with, again,  $1/\log N$  corrections, which we numerically confirm in Fig. 4(a). The full Lyapunov spectrum, on the other hand, gets flatter for larger  $N$  and we observed the emergence of the  $\Delta\lambda(h) \sim 1/\sqrt{N}$  scaling [Fig. 4(b)], but we are currently unable to study the larger systems, in order to overcome finite-size effects to obtain clear evidence of  $\mathcal{O}(\log N)$  subextensive LEs. Nevertheless, it is already clear from Fig. 4(b) that the  $h$  domain where the  $1/\sqrt{N}$  scaling holds widens with  $N$ , suggesting a flat (zero-valued) extensive part with a subextensive, possibly logarithmic, band of positive LEs.

We finally examine the influence of collective chaos on our results, an important generic case for dissipative globally coupled systems [3]. Lyapunov spectra then contain modes governing the macroscopic dynamics, whose associated covariant Lyapunov vectors are delocalized [6]. In the case of globally coupled limit-cycle oscillators,  $\dot{W}_j = W_j - (1 + ic_2)|W_j|^2 W_j + K(1 + ic_1)(\langle W \rangle - W_j)$ , with complex variables  $W_j$ ,  $\langle W \rangle \equiv \frac{1}{N} \sum_j W_j$ ,  $c_1 = -2.0$ ,  $c_2 = 3.0$ , and  $K = 0.47$ , the largest LE is such a collective mode [6]. Here we see that it does not obey Eq. (4) for  $N$  large enough while the following, “noncollective” LEs do [Fig. 4(d)]. This result comforts the general picture of the macroscopic modes being present but asymptotically decoupled from the other ones in Lyapunov spectra, whether in the bulk or in the subextensive layers.

Our findings recall the importance of the order of limits in systems with long-range interactions: For the ferromagnetic phase of the HMF model for instance, considering

directly the infinite-size system (the Vlasov equation [8]), one misses the fact that residual but influential chaos remains in the  $N \rightarrow \infty$  limit, even though the bulk exponents vanish asymptotically. The Lyapunov modes in the subextensive layers capture “extreme events” in phase space, much like the largest LE in locally coupled systems [16,17]. For the HMF case, this is particularly clear since, whereas the covariant vectors for bulk LEs are carried by typical oscillators, the first Lyapunov vector is localized on those oscillators currently in the vicinity of the separatrix, the most unstable part of (local) phase space [Fig. 4(c)]. Even though they are in logarithmic numbers and localized on special regions of phase space, the Lyapunov modes of the subextensive layers may have an important impact on macroscopic properties, such as the thermodynamic entropy of Hamiltonian systems [18].

In summary, we have shown that microscopic chaos in systems made of  $N$  globally coupled dynamical units exhibits a rather peculiar form of extensivity: their Lyapunov spectrum  $\lambda(h)$  is asymptotically flat, thus “trivially” extensive, but sandwiched between subextensive bands with LEs taking different values. In the presence of macroscopic dynamics, the corresponding collective Lyapunov modes are just superimposed on this structure. The bulk LEs converge as  $\lambda(h) \simeq \lambda_0 + \text{const}/\sqrt{N}$  to the value  $\lambda_0$  given by a single dynamical unit forced by the mean field. In contrast, the subextensive layers contain  $\mathcal{O}(\log N)$  LEs whose values vary as  $\lambda \simeq \lambda_\infty + \text{const}/\log N$  with  $\lambda_\infty \neq \lambda_0$ . Investigating further the genericity of our results and providing a theoretical basis to the  $1/\sqrt{N}$  scaling of bulk LEs and the  $\log N$  size of subextensive bands are important tasks left for future study.

- 
- [1] *Dynamics and Thermodynamics of Systems with Long-Range Interactions*, edited by T. Dauxois *et al.*, Lecture Notes in Physics Vol. 602 (Springer-Verlag, Berlin, 2002).
  - [2] Y. Kuramoto, *Chemical Oscillations, Waves, and Turbulence* (Dover, New York, 2003).
  - [3] T. Shibata and K. Kaneko, *Phys. Rev. Lett.* **81**, 4116 (1998); M. Cencini *et al.*, *Physica (Amsterdam)* **130D**, 58 (1999); N. Nakagawa and Y. Kuramoto, *ibid.* **75D**, 74 (1994); S. Olmi, A. Politi, and A. Torcini, *Europhys. Lett.* **92**, 60007 (2010).
  - [4] D. Ruelle, *Commun. Math. Phys.* **87**, 287 (1982).
  - [5] See, e.g., M.R. Paul *et al.*, *Phys. Rev. E* **75**, 045203(R) (2007), and references therein.
  - [6] K. A. Takeuchi, F. Ginelli, and H. Chaté, *Phys. Rev. Lett.* **103**, 154103 (2009).
  - [7] M. Antoni and S. Ruffo, *Phys. Rev. E* **52**, 2361 (1995).
  - [8] T. Dauxois *et al.*, in Ref. [1], p. 458.
  - [9] M.-C. Firpo, *Phys. Rev. E* **57**, 6599 (1998).
  - [10] S. Tănase-Nicola and J. Kurchan, *J. Phys. A* **36**, 10299 (2003).
  - [11] V. Latora, A. Rapisarda, and S. Ruffo, *Physica (Amsterdam)* **131D**, 38 (1999); G. Miritello, A.

- Pluchino, and A. Rapisarda, *Europhys. Lett.* **85**, 10007 (2009); T. Manos and S. Ruffo, [arXiv:1006.5341v2](https://arxiv.org/abs/1006.5341v2).
- [12] For RM and GCM, LEs are estimated typically over  $10^6$  time steps after a  $10^5$  transient for the trajectory and a  $100N$  equilibration of vectors. For HMF, these numbers are, in natural time units,  $2 \times 10^7$ ,  $4000N$ , and  $2000N$ .
- [13] Note that coupling effect for two dynamical units was studied in H. Daido, *Prog. Theor. Phys. Suppl.* **79**, 75 (1984), which reported a shift of  $\lambda$  by  $|1/\log\epsilon|$ .
- [14] For GCM, the scaling  $\Delta\lambda \sim 1/\sqrt{N}$  for the bulk LEs is not fully established at the largest size we could reach.
- [15] F. Ginelli *et al.* (to be published).
- [16] H. Chaté, *Europhys. Lett.* **21**, 419 (1993).
- [17] D. A. Egolf *et al.*, *Nature (London)* **404**, 733 (2000).
- [18] M. Dzugutov, E. Aurell, and A. Vulpiani, *Phys. Rev. Lett.* **81**, 1762 (1998); S. I. Sasa and T. S. Komatsu, *ibid.* **82**, 912 (1999).